Jakub Chmielecki, Grzegorz Liśkiewicz*, Władysław Kryłłowicz

Numerical study of surge predecessors in centrifugal blower — inlet recirculation

Institute of Turbomachinery, Lodz University of Technology,
219/223 Wólczańska, 90-924 Łódź, Poland

Abstract

Paper presents the numerical investigation of inlet recirculation in a centrifugal blower. This phenomenon is known as a local flow instability that is not too harmful in centrifugal compressors compared to centrifugal pumps. However recent findings have shown that it can be regarded as a surge predecessor, and hence very significant for compressors. Therefore there is strong need to understand its physics. One of ways to understand it to apply computational fluid dynamic (CFD) simulations. Therefore in this study the transient numerical simulations were conducted and results were related to the experimental data presented in other papers. Simulation confirmed that the inlet recirculation structure can be resolved by means of CFD and the results are in agreement with some available models. Inlet recirculation structure built up gradually along the circumference increasing the power loss. Obtained structure also explained pressure variations observed in experiments. This has shown that CFD can bring significant improvement in existing antisurge systems and recirculation bleeds that extend the machine operating range.

Keywords: Centrifugal; Compressor; Blower; CFD; Inlet recirculation

1 Introduction

1.1 Inlet recirculation in centrifugal compressors

Inlet recirculation is a phenomenon that has been initially discovered and examined for low specific speed centrifugal pumps in late 70's and early 80's. Main

---

*Corresponding Author. Email adress: grzegorz.liskiewicz@p.lodz.pl

contributions at this time were done by Breugelmans, Sen, and Schiavello [1–3], Tanaka [4], and Fraser [5]. Yet, it was not examined widely in centrifugal compressors. This is perhaps due to the fact that inlet recirculation is regarded as relatively harmless to machines operating with low density fluids. This is true, but recently some attention was drawn to the fact, that this phenomenon can be treated as a crucial pre-surge indicator [6–9].

In Fig. 1 meridional cross-section of centrifugal compressor affected by the inlet recirculation phenomenon is presented [10]. It can be clearly seen that the effective channel intake is considerably smaller than that in the nominal conditions. Inlet recirculation takes the form of three dimensional self-contained toroidal structure.
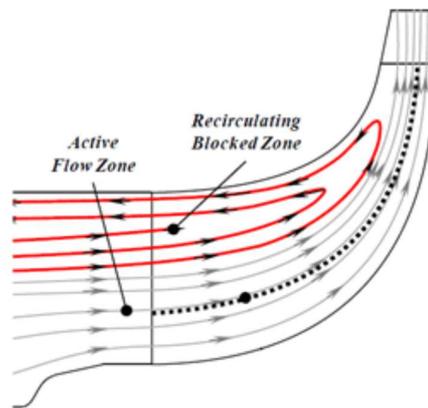

Figure 1: Meridional cross-section with the streamlines in presence of inlet recirculation.

Most commonly, the effect of inlet recirculation is included in compressor design together with outlet recirculation as a loss coefficient or slip factor that depends on mass flow rate [10–13]. At design and over-design conditions it is normally neglected whereas at under-design condition it depends on mass flow rate. The character of this dependency has not been definitely established, however, most of above mentioned models agree that the losses increase dramatically around 0.3–0.5 of design mass flow rate.

Another question considers the inlet recirculation inception conditions and mechanism. Some general statements concerning pumps were drawn by Gulich [14] and could be suspected to be valid also for compressors. He postulated that the inlet recirculation onset is possible when two conditions are fulfilled:

- the flow must separate, locally,
- strong pressure gradients must develop perpendicular to the direction of the main flow.

1.2   Should inlet recirculation be suppressed?

Inlet recirculation can be passively suppressed by application of casing bleed or casing system tested among others by Hunziker *et al.* [15], Tamaki *et al.* [6,16] or Yang *et al.* [17]. They examined different recirculation channels that direct recirculated flow out of the impeller eye and allow to obtain considerable broadening of the compressor map without big efficiency cost.

Inlet recirculation was also proven to have great potential in antisurge systems applications. McKee *et al.* [18] used a drag probe introduced to the impeller intake to collect axial strain signals. As the compressor approached surge, the negative force acting on the probe was increasing. Constructing antisurge system based on this force signal allowed to obtain up to 35.5% increase in operating range comparing to different controllers [19]. Furthermore, it was concluded that the aforementioned changes in the flow pattern are repeatable under various conditions and can be standardized for the application across multiple types of centrifugal compressors.

Both abovementioned inlet recirculation based concepts have still much room for improvement. The main reason lies in fact, that still not much is known about the IR flow physics and inception mechanism. One of ways of achieving this aim may include use of computational fluid dynamics (CFD). This method was not exhaustively employed for this purpose. It is not known, if it would be possible to obtain CFD model of the inlet recirculation with confidence and resolution allowing for further progress.

1.3   Aim of study

The aim of this study is to validate whether it is possible to resolve a 3D representation of the inlet recirculation flow physics by means of CFD. If yes, then the initial statements will be drawn about possible conclusions and ways in which this method can be used for antisurge devices.

2   Method

A centrifugal blower DP1.12 was investigated, where inlet recirculation was observed in experimental study [20,21]. While the stand geometry is fully described in abovementioned paper, this section is devoted to numerical method that was chosen to assure best reproduction of physical conditions met in the experimental study.

2.1 Blower description

Full description of the DP1.12 blower can be found in [20,21] together with its performance curve. The inlet pipe of diameter 300 mm is followed by the Witoszynski nozzle and the impeller with 23 blades, vaneless diffuser and circular volute. The rotor inlet diameter at the hub and the inlet span equals 86.3 mm and 38.9 mm, respectively. At the outlet those values changed to 330 mm and 14.5 mm. The diffuser outlet diameter is equal to 476 mm. The volute radius in experimental stand is gradually increasing streamwise from the volute tongue gap of 5 mm towards the outlet pipe of diameter 150 mm. Due to the fact, that this simulation was focused on impeller inlet, the volute was not included in this study. However, it is known that volute performance can have little influence even on inlet zone [22]. Therefore, after obtaining satisfactory CFD representation of the inlet recirculation, the next approach could include examination of the volute influence.

2.2 Computational domain

Computational domain included Witoszynski nozzle inlet (Fig. 2) and full annulus of 23-bladed impeller (Fig. 3) with vaneless diffuser. The number of nodes and elements for each domain is presented in Tab. 1. It is conspicuous that elements number in case of the impeller domain is dozens of times bigger than in inlet nozzle domain although the absolute volume of the first one is smaller. This is due to the fact that instable phenomena were expected to appear at the impeller inlet, where mesh was most refined as well as in the blades boundary layers. Inlet nozzle mesh, on the other hand, has been mainly used to move away inlet boundary conditions from the examined region thus making the simulations less stiff. All mesh elements had skewness over 0.38 and aspect ratio below 0.91. With exclusion of boundary layer cells the maximum aspect ratio was below 0.5. Both domains utilized hexagonal cells. Stretching of the hexahedral elements has been aligned with the flow direction which usually produces smaller numerical diffusion [23].

2.3 Simulation setup

Both domains have been defined with similar domain setup. The fluid was set to air ideal gas and the domain motion was set to rotating with the angular velocity of 100 Hz. This required application of counter rotating wall in inlet nozzle. It was selected as better tradeoff allowing to avoid interface with sliding mesh on boundary located close to the inlet recirculation zone. The reference pressure was set to 1 atmosphere and turbulence model was set to k-ε which is typical
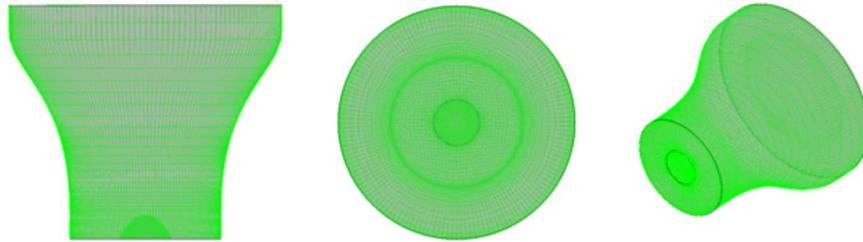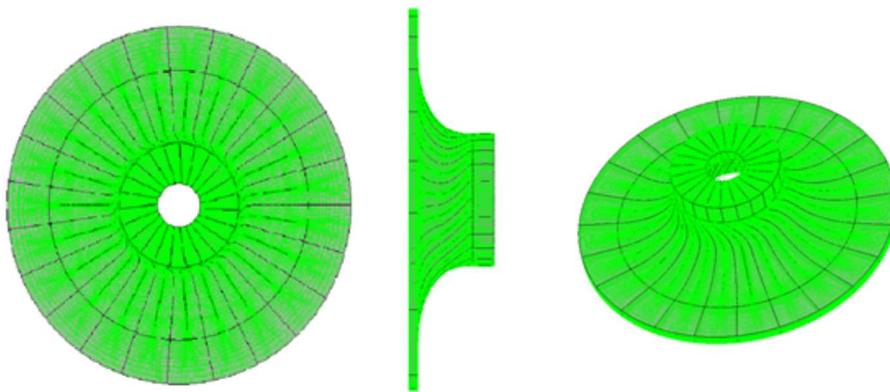
Figure 2: Inlet nozzle domain overview.

Figure 3: Blower and diffuser domain overview.

Table 1: Mesh overview.

Overall	
Number of nodes	2.7×10^6
Number of elements	2.9×10^6
Inlet nozzle	
Number of nodes	0.2×10^6
Number of elements	0.2×10^6
Impeller	
Number of nodes	2.5×10^6
Number of elements	2.7×10^6

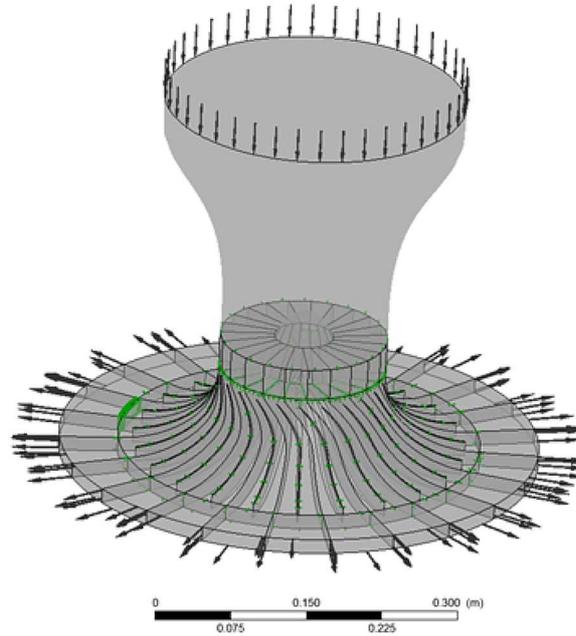turbulence model applied for studies of unstable flows in centrifugal compressors [24–26].

Figure 4: Boundary conditions overview.

In Fig. 4 overview of the boundary conditions applied to the simulated compressor is presented. Since presurge instabilities that appear in the compressor are inherently three dimensional, no symmetry condition has been applied; all 23 passages have been simulated.

2.4   Boundary conditions

Inlet nozzle

Static frame total pressure was placed with the relative pressure value of 0 Pa. A flow direction has been defined as normal to boundary condition and heat transfer option was set to static frame total temperature of 20 °C. The incoming turbulence level was set to 5%. On the outer walls of the domain a rotating wall boundary was placed with wall velocity defined as counter rotating wall. Hub tip was set as an ordinary wall. Both walls were considered adiabatic throughout simulations. At the outlet of the inlet nozzle domain an interface was placed, transferring results to the inlet section domain.

Inlet section

Inlet section domain – being a subdomain of the blower – was defined from both sides with the interfaces transferring results from the inlet nozzle domain and to the compressor domain, respectively. Outer wall was set as a counter-rotating wall, whereas hub was set as a static wall in mesh domain. Both walls were considered adiabatic throughout the simulation.

Impeller

Blades in the impeller domain were defined as a static, no slip, adiabatic walls. Hub and shroud were defined as static and counter-rotating wall, respectively. The clearance between blade tips and shroud was implemented by means of interface.

Diffuser

Both walls of the vaneless diffuser were defined as counter-rotating, smooth walls with no heat transfer. At the outlet of the diffuser a fixed mass flow rate was set adequately to analyzed case.

3   Solver control

The convergence criteria for average momentum and mass flow rate residuals of all of the simulations have been set on the level of 10^{-4}. Such solutions are good enough to reveal general trends and flow structures that arise within the compressor during presurge stages.

Based on results of [21,27] it was expected that the inlet recirculation may appear for mass flow rate between 0.5 kg/s and 0.1 kg/s, hence several cases were examined in this region. However, at mass flow rates smaller than 0.25 kg/s the simulation did not converge to assumed level and hence all of the simulations have been set as steady state at first. In case of high fluctuations a transient simulation have been set, using steady state results as an input initial condition. The time step for the nonsteady simulations has been fixed with the value of 0.000088 s. Given nominal rotational speed of the blower one time step corresponded to the impeller rotation by 1/5 of the passage.

4 Results

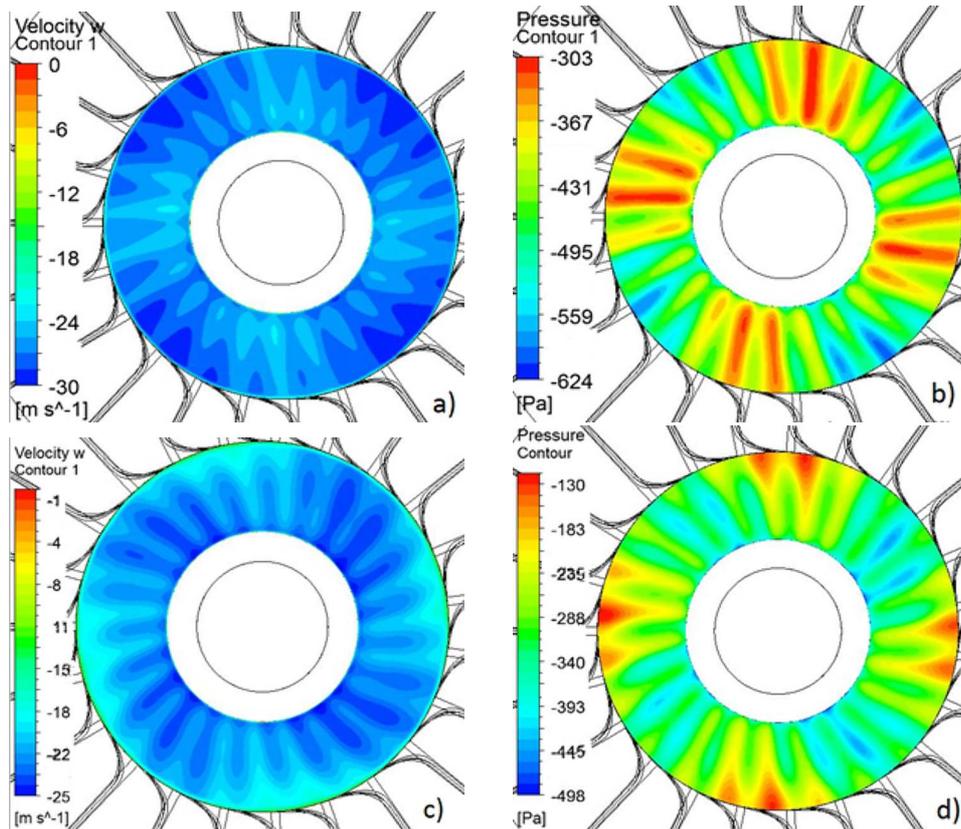## 4.1 Before inlet recirculation (0.5 kg/s and 0.4 kg/s)

Figure 5: Top view of the compressor intake for mass flow rate of 0.5 kg/s: a) normal velocity; b) gauge pressure and mass flow rate 0.4 kg/s; c) normal velocity; d) gauge pressure.

In Fig. 5 contour plots of the cross-section placed in the proximity of the inlet have been shown. In terms of both velocity and pressure field some irregularities can be observed on the intakes for both mass flow rates. For mass flow rate 0.5 kg/s, in case of the velocity field there exist four zones of higher in-flow velocity of about 30 m/s whereas at any other place normal in-flow velocity does not exceed 25–27 m/s. For mass flow rate 0.4 kg/s flow structures are very similar but the velocity values attain about 25 m/s for the high speed zones and about 17 m/s for the low speed ones, respectively.

The aforementioned flow structure is also expressed at the pressure plot – four high-pressure zones and four low-pressure zones are observed. The gauge pressure is higher where the inlet velocity is lower.

4.2   Inlet recirculation onset (0.35 kg/s and 0.3 kg/s)

Since previous simulations have shown irregular intake velocity patterns it was suspected that inlet recirculation phenomenon could arise at mass flow rates higher than 0.3 kg/s. Therefore, it was decided to introduce a middle value of the flow to catch structures associated with origins of the inlet recirculation. A simulation with the outflow value from the diffuser of 0.35 kg/s has been thus set. Due to high residuals in steady simulation, a computation was changed to transient scheme.
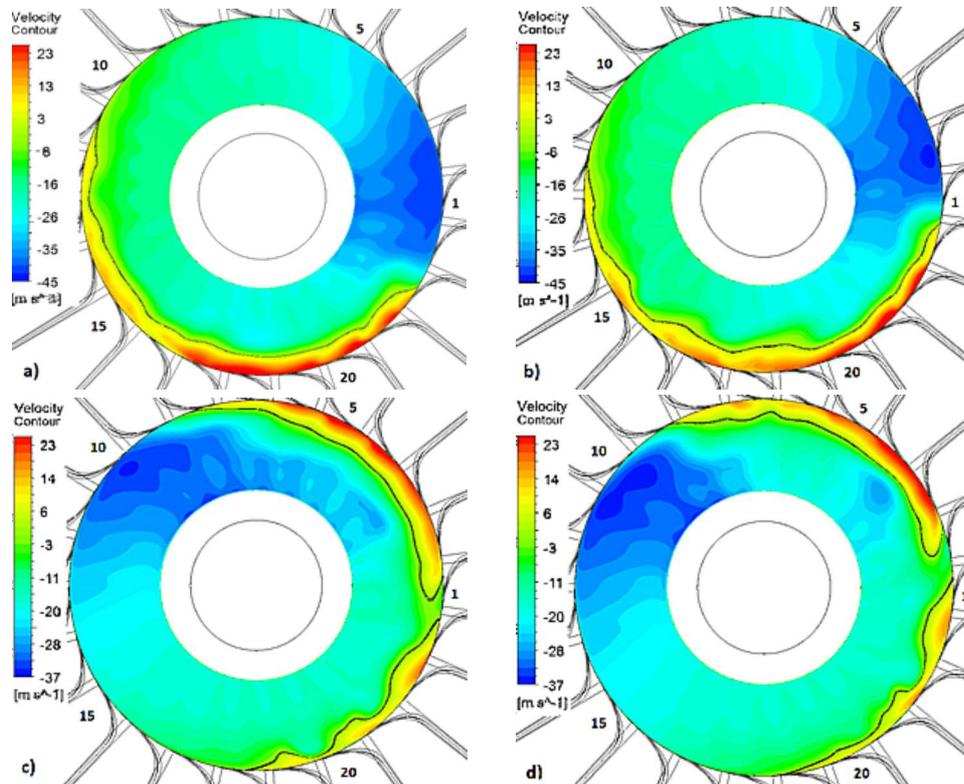

Figure 6: Top view of the compressor intake for mass flow rate of 0.35 kg/s at times: τ (a), and $\tau + 0.0044$ s (b), and for mass flow rate of 0.3 kg/s at times τ (c), and $\tau + 0.0044$ s (d).

In Fig. 6 normal velocity field at the cross section close to the impeller intake is presented at times τ, and $\tau + 0.0044$ s for mass flow rate of 0.35 kg/s (Figs. 6a and 6b) and 0.3 kg/s (Figs. 6c and 6d), respectively. Solid lines in the figures represent region where inlet normal velocity equals to 0; flow behind these lines is therefore recirculating, having direction opposite to the bulk flow. As it was mentioned earlier both flow conditions presents very similar normal velocity intake pattern. It can be seen that in every case recirculation zone encirculates about half of the inlet circumference; it is also observable that it is slightly more noticeable in case of the 0.3 kg/s mass flow rate. Furthermore, in each case high-velocity zone can be observed ahead of the recirculating zone, where the intake velocity reaches up to 45 m/s and 37 m/s values for mass flow rate of 0.35 kg/s and 0.3 kg/s, respectively. These values are much higher than those within other intake regions.

In Fig. 6 propagation of this structure after 0.0044 s (that corresponds to 50 timesteps and 44% of full impeller rotation) is presented for the 0.35 kg/s and 0.3 kg/s mass flow rate conditions. It is observable that the inlet recirculation cell has slightly different position in each case. It is also visible that high-velocity zone is propagating behind the inlet recirculation in the same direction. What differs those two cases is the size and the regularity of the recirculated flow. In case of the smaller mass flow rate the size of inlet recirculation is bigger and it seems to fluctuate more strongly from time step to time step. It also splits and merges into two inlet recirculation zones as the simulation progress. Hence, smaller mass flow rate case appears to be less stable although the inlet pattern is very similar.

In order to examine the root of the phenomenon that occurs at the inlet, flow through the impeller and diffuser have been investigated. In the Fig. 7 blade-to-blade view of the mid section between hub and shroud is shown for time steps splitted by 0.0044 s interval for 0.35 kg/s mass flow rate. Mass flow rate of 0.3 kg/s is not exposed since the general flow pattern appears the same; differences lays in smaller velocity absolute values which can be attributed to smaller mass flow rate. Velocity field is strongly irregular from channel to channel. It can be seen that in channels 1–5 (Fig. a) and 2–6 (Fig. b) are not affected by secondary flows. In the next consecutive channels there exist transient state; channels are getting more and more stagnated with the stagnation zones extending closer to the blade tip. Finally in case of the 13–22 (Fig. 7a) and 13–21 (Fig. 7b) stagnation zones cover almost totally suction side of the blade.
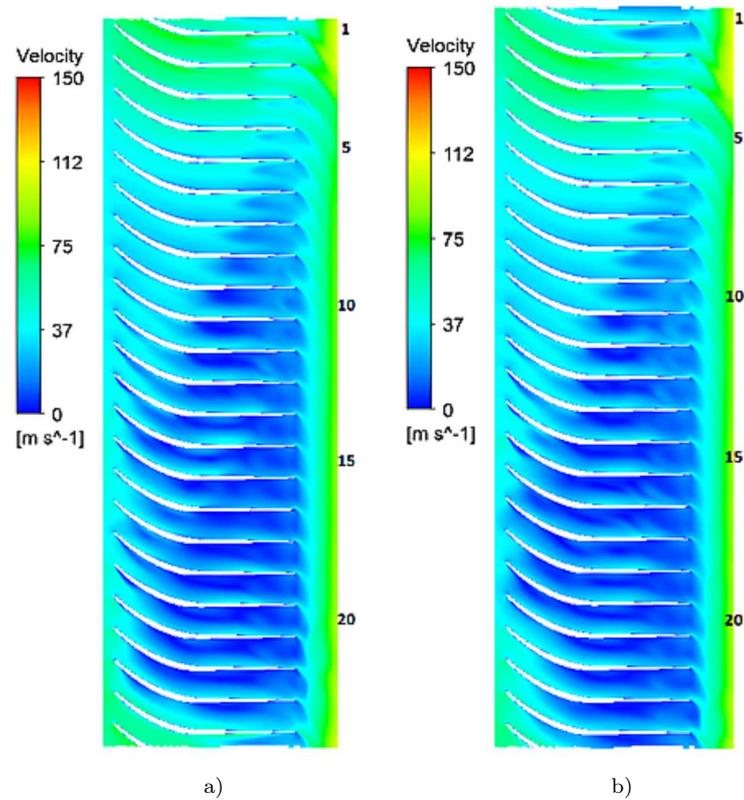
Figure 7: Blade-to-blade at the half way between hub and shroud velocity field for mass flow rate of 0.35 kg/s at times: a) τ s, and b) $\tau + 0.0044$ s.

4.3 Developed inlet recirculation (0.25 kg/s)

In this case the obtained inlet recirculation structure was highly time-dependent. Going through the different time steps it was noticed that what at first appeared as a stationary instability begins to change after a few impeller rotations.

At the beginning of the simulation regular pattern of the inlet recirculation could be observed (Fig. 8a) on the circumference of the compressor intake. This pattern can be regarded as approximately axis-symmetric with the normal inlet velocity values varying from the -21 m/s in the proximity of the hub to 13 m/s at the intake outer circumference. In the further time steps observable intake velocity distribution begins to shift towards less stable one. In Fig. 8b inlet velocity field is presented for the time τ, after the time step exposed at Fig. 8a.

Observable velocity profile is strongly irregular and far from being axis-symmetric. Recirculation zones occupy major part of the outer ring, though there exist places where the bulk flow remains unaffected. Velocity ranges from -30 m/s to 28 m/s with the peak values located very close to each other. At the time step $\tau+0.0044$ s (Fig. 8c) velocity profile is very different. Although the general pattern appear the same, inlet recirculation distribution differs strongly, i.e., the observed behavior is changing with the high frequency. In order to check flow structures in the impeller and diffuser again, blade-to-blade view has been examined.
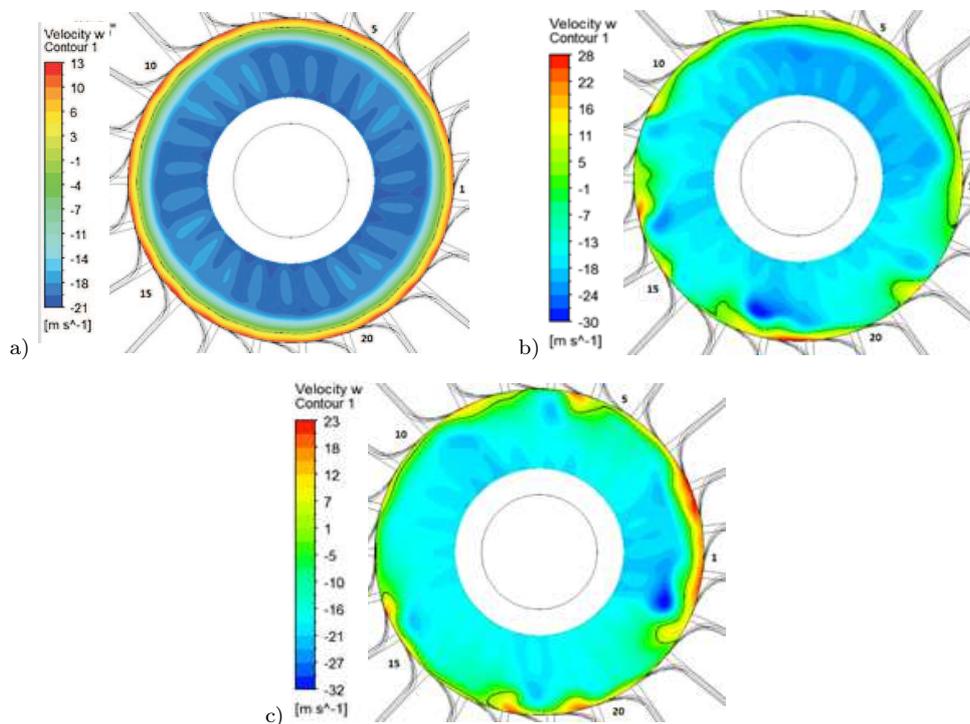

Figure 8: Top view of the compressor intake for mass flow rate of 0.25 kg/s at times: a) 0; b) τ s; c) $\tau + 0.0044$ s.

In Fig. 9 blade-to-blade views of the midsections between hub and shroud have been exposed for three different time steps: 0, τ, and $\tau+0.0044$ s ($\tau > 0$). Initially, at time 0 s (Fig. 9a), velocity distribution is regular from channel-to-channel with the stagnation zones appearing in the middle part of the suction side of the blade. In each channel inlet a smooth shade behind the tip exists, i.e., leading edge flow separation occurring due to nonnominal angle of attack.
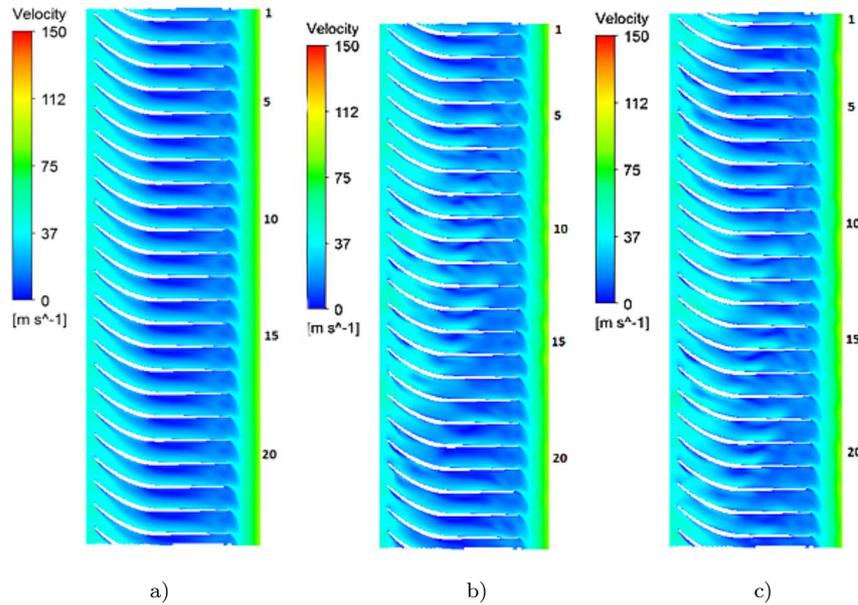
Figure 9: Blade-to-blade velocity distribution for mass flow rate of 0.25 kg/s at times: a) 0 s, b) τ, and c) $\tau + 0.0044$ s.

5   Discussion

Although it is clear that no recirculation pattern was observed at flow rates 0.5 kg/s and 0.4 kg/s, nonregularity at the impeller inlet can have some correlation to this phenomenon. Typical compressor intake velocity-pressure pattern is axisymmetrical with the pattern of 23 passages reflected within it. Here, one could observe a circumferential distortion or pressure and velocity field.

In case of flow rates 0.35 kg/s and 0.3 kg/s the inlet recirculation structure became visible. Knowing that nominal mass flow rate of this machine is 0.8 kg/s, one could state that the inlet recirculation onset is located around ratio $\frac{\dot{m}}{\dot{m}_D} \approx 0.43$ which is quite high, but still in the region predicted by most of models used in meanline modeling [10–13]. It is much earlier that the Augier prediction [13] (about 0.37), but still in good agreement with Oh *et al.* or Qiu *et al.* [11,12]. It has to be noted that current findings show that the inlet recirculation does build up gradually along the circumference. This again confirms models of Oh *et al.* or Qiu *et al.* [11,12], where loss factor increases gradually without any critical value. For 0.35 kg/s and 0.3 kg/s high speed zones appearing behind inlet recirculation cells are noticeable. By comparing with blade-to-blade plot (Fig. 7) one could see

that these regions correspond to the clear channels within the impeller. As, circumferentially, velocity starts to decrease, channels are getting stagnation zones more and more developed, starting from the blade part closer to the diffuser. For both presented time steps, channel in which recirculation begins (moving counter clockwise) corresponds to the first channel (12 and 13 for τ and $\tau + 0.0044$ s, respectively) in which stagnation zone seems to touch the blade tip causing separation on the suction side of the blade. In the case of 0.25 kg/s there are no obvious pattern to connect inlet flow conditions with blade-to-blade plot in neither $t = \tau$ nor $t = \tau + 0.0044$ s. In this case the impeller flow patterns seem to be placed randomly independent of the intake structures. As it was noticed, the changes here occur very quickly, it may therefore be the case that one of the flow structures is lagging behind the other.

At 0.25 kg/s the inlet recirculation at some time took the form of the toroid, well-known from the literature [2,5,14]. However, even at this condition this structure was not permanent and very soon lost its axial symmetricity. This may confirm the fact observed in [27], that the inlet recirculation was connected with very large pressure jumps caused by appearance and disappearance of the recirculation zone at given location. This also explains the random nonperiodic character of these oscillations observed also beforehand [28].

6   Summary and coclusions

Conducted study examined compressor intake flow patterns in DP1.12 centrifugal blower for several mass flow rates: 0.5 kg/s, 0.4 kg/s, 0.35 kg/s, 0.3 kg/s, and 0.25 kg/s. All of these were been chosen to find out how the recirculation phenomenon initiated and how it is associated with the flow throughout the impeller. After analyzing the results, three intake flow structures could be distinguished:

- For flow values of 0.5 kg/s and 0.4 kg/s steady state simulations revealed no inlet recirculation although some circumferential fluctuations in both pressure and velocity fields were observed.
- Flow values of 0.35 kg/s and 0.3 kg/s showed intake pattern in which part of the inlet circumference was affected by the recirculating flow. It is conspicuous that as the flow decreased (from 0.35 to 0.3) recirculation zone affected greater part of the circumference.
- The last inlet flow structure was observed in case of the 0.25 kg/s mass flow rate where highly unsteady inlet recirculation was noticeable affecting the whole outer circumference of the intake.

It can be concluded that inlet recirculation started as the highly dynamic instability. Although it is usually referred as being dynamically stable, computed simulations showed that inlet recirculation started in form of the recirculation zone of the parabolic shape located along the portion of the circumference. As the flow decreased, the phenomenon strengthen and started to affect greater and greater part of the circumference while simultaneously becoming less stable. Apparently, inlet recirculation can be linked to the flow structures in the impeller. It can be believed that in simulated cases recirculation took place when the stagnation zones present in the impeller touched the tip of the suction side of the blades. This, could not be observed in case of the 0.25 kg/s outflow, presumably because of the highly dynamic form of the inlet recirculation instability which could trigger lagging of inlet flow structure behind the impeller flow or vice versa.

References

[1] Sen M., Breugelmans F., Schiavello B.: *Reverse flow, prerotation and unsteady flow in centrifugal pumps.* In: Proc. NEL Fluid Mechanics Silver Jubilee Conf. Glasgow 1979.

[2] Breugelmans F.A., Sen M.: *Prerotation and fluid recirculation in the suction pipe of centrifugal pumps.* In: Proc. 11th Turbomachinery Symp., 1982, 165–180.

[3] Schiavello B., Sen M.: *On the prediction of the reverse flow onset at the centrifugal pump inlet.* ASME Symp. on Performance Prediction of Centrifugal Pumps and Compressors, New Orleans 1980.

[4] Tanaka T.: *An experimental study of backflow phenomena in a high specific speed propeller pump.* Proc. ASME, 80-FE–6, 1980.

[5] Fraser W.H.: *Recirculation in centrifugal pumps.* In: Proc. Construction of Fluid Machinery and Their Relationship to Design and Performance, World Pumps, 1981, 65–86.

[6] Tamaki H.: *Experimental study on surge inception in a centrifugal compressor.* Int. J. Fluid Mach. Sys. **2**(2009), 4, 409–417.

[7] Liskiewicz G., Horodko L.: *Time-frequency analysis of the surge onset in the centrifugal blower.* Open Eng. **5**(2015), 1, 299–306.

[8] Kabalyk K., Liśkiewicz G., Horodko L., Stickland M., Kryłowicz W.: *Use of pressure spectral maps for analysis of influence of the plenum volume on the surge in centrifugal blower.* Proc. ASME, 2014, GT2014–26931.

[9] Horodko L.: *Investigation of centrifugal compressor surge with wavelet methods.* In: Proc. 6th Eur. Conf. on Turbomachinery, Fluid Dynamics and Thermodynamics Vol. 2, Lille 7–11 March, 2005, 635–644.

[10] Harley P., Spence S., Filsinger D., Dietrich M., Early J.: *Meanline modelling of inlet recirculation in automotive.* ASME Turbo Expo 2014: Turbine Technical Conference and Exposition, Vol. 2D: Turbomachinery, Düsseldorf, June 16–20, 2014, GT2014-25853, V02DT42A020.

[11] Qiu X., Japikse D., Anderson M.: *A meanline model for impeller flow recirculation.* Proc. ASME Turbo Expo, GT2008–513, 2008.

[12] Oh H.W., Yoon E.S., Chung M.K.: *An optimum set of loss models for performance prediction of centrifugal compressors.* P I Mech. Eng. A-J Pow. **211**(1997), 4 , 331–338.

[13] Aungier R.H.: *Centrifugal Compressors: A Strategy for Aerodynamic Design and Analysis.* ASME Press, 2000.

[14] Gülich J.F.: *Centrifugal Pumps.* Springer, Berlin Heidelberg 2014.

[15] Hunziker R., Dickmann H.-P., Emmrich R.: *Numerical and experimental investigation of a centrifugal compressor with an inducer casing bleed system.* P I Mech. Eng. A-J Pow. **215**(2001), 6, 783–791.

[16] Tamaki H., Unno M., Tanaka R., Yamaguchi S., Ishizu Y.: *Enhancement of centrifugal compressor operating range by control of inlet recirculation with inlet fins.* J. Turbomach. **138**(2016), 10, 01010-1–01010-12

[17] Yang M., Zheng X., Zhang Y., Bamba T., Tamaki H., Huenteler J., Li Z.: *Stability improvement of high-pressure-ratio turbocharger centrifugal compressor by asymmetric flow control — Part I: Non-axisymmetrical flow in centrifugal compressor.* J. Turbomach. **135**(2013), 3, 1–9.

[18] McKee R.J., Edlund C.E.: *Method and Apparatus for Detecting the Occurrence of Surge in a Centrifugal Compressor.* Google Patents, 2006.

[19] McKee R.J., Siebenaler S.J., Deffenbaugh D.M.: *Increased flexibility of turbo-compressors in natural gas transmission through direct surge control.* U.S. Department of Energy Report, San Antonio 2005.

[20] Liśkiewicz G., Horodko L., Stickland M., Kryłłowicz W.: *Identification of phenomena preceding blower surge by means of pressure spectral maps.* Exp. Therm. Fluid Sci. **54**(2014), 267–278.

[21] Garcia D., Stickland M., Liskiewicz G.: *Dynamical system analysis of unstable flow phenomena in centrifugal blower.* Open Eng. **5**(2015), 1, 332–342.

[22] Sorokes J.M., Borer C.J., Koch J.M.: *Investigation of the circumferential static pressure non-uniformity caused by a centrifugal compressor discharge volute.* In: Proc. Int. Gas Turbine and Aeroengine Cong., 98-GT-326, 1998, 1–9, doi:10.1115/98-GT-326.

[23] Ansys Fluent 14.0 Theory Guide. ANSYS Inc, 2011.

[24] Guo Q., Chen H., Zhu X.-C.C., Du Z.-H.H., Zhao Y.: *Numerical simulations of stall inside a centrifugal compressor.* J. Power Energ. **221**(2007), 5, 683–693.

[25] Huang W., Geng S., Zhu J., Zhang H.: *Numerical simulation of rotating stall in a centrifugal compressor with vaned diffuser.* J. Therm. Sci. **16**(2007), 2, 115–120.

[26] Turunen-Saaresti T., Larjola J.: *Unsteady pressure field in a vaneless diffuser of a centrifugal compressor: An experimental and computational analysis.* J. Therm. Sci. **13**(2004), 4, 302–309.

[27] Liśkiewicz G., Horodko L., Stickland M., Kryłłowicz W.: *Identification of phenomena preceding blower surge by means of pressure spectral maps.* Exp. Therm. Fluid Sci., **54**(2014), 267–278.

[28] Horodko L.: *Detection of surge precursors in a centrifugal compressor with a wavelet method.* In: Proc. 7th Eur. Conf. on Turbomachinery, Fluid Dynamics and Thermodynamics, Athenes 2007, 317–326.